44th AIAA Aerospace Sciences Meeting and Exhibit, 9-12 Jan 2006, Reno, Nevada

Preliminary Experiments of Barrier Discharge Plasma Actuators using Dry and Humid Air

Richard Anderson* and Subrata Roy†

Test Facility, Computational Plasma Dynamics Laboratory, Kettering University, Flint, MI 48504

Experiments are performed using dry and humid air to ascertain the effect of humidity on the performance of a plasma actuator in flight conditions. These actuators are becoming popular in controlling flow about low to moderate speed aerospace vehicles. These experiments are performed at a new Test Facility of the Computational Plasma Dynamics Laboratory (CPDL) in Kettering University. A blow-down open loop wind tunnel with 1-foot by 1 foot test section is used for a range of flow speeds. Our aim is to complement the ongoing numerical modeling effort at CPDL with test data for validation purposes. Preliminary measurements are made from the pressure profile of the base-geometry/DBD actuator in each test condition. Initial calculations of the theoretical Blasius skin-friction are made. The coefficients of those values are reported. Recommendations for use of the plasma actuator based on our initial findings are also presented.

1. Introduction

THE dielectric barrier discharge (DBD) actuator is a device that shows tremendous potential for use in aerospace applications across a range of speed and altitude regimes. It has the advantages of rapid response, elimination of moving parts, low power draw, and due to its solid-state nature it may reduce drag considerably [1]. The actuator has been shown to be an effective device for controlling airflow [2]. However, to date measurements have not been openly reported to determine the effect of humidity upon DBD actuators.

In order for this family of devices to gain widespread acceptance in the aircraft industry and to replace the mechanical systems currently in use, they must be shown to be capable of all-weather flight in a wide variety of climates. It has long been assumed that heavy humidity, at levels one may expect at airports in or near the tropical belt, inhibits the operation of the DBD device [3]. Indeed, experiments performed in 2003 [4] were made at a pressure of 750 ± 25 Torr and humidity as high as 14%. However, the lowest relative humidity (RH) presented in this paper is over 40%.

These experiments are performed at a new high voltage Test Facility of the Computational Plasma Dynamics Laboratory (CPDL) in Kettering University. While traditional experiments [1-4] were performed using RF applied electrode voltage, the frequency for this paper was set to a low 60 Hz. It has been found [5] that an ideal frequency exists for any particular unsteady forcing frequency. However, this paper deals only with a constant, steady frequency, as opposed to a duty cycle or beat frequency

This paper documents a preliminary set of investigations into the effects of humid air on DBD actuators, and tries to provide some possible recommendations for the use of them in operational settings.

2. Experimental Setup

2.1 Wind Tunnel and Instrumentation

Recently, in 2005, a high voltage plasma flow Test Facility was built at Kettering University to perform physical experimentations that will complement the ongoing numerical developments at CPDL with test data for validation purposes. The Test Facility consists of an open-loop blow-down wind tunnel with a 1-foot x 1-foot test section. The tunnel was constructed according to the principles shown by Mehta and Bradshaw in 1979 [6]. A variable-speed 10500 CFM axial-fan blower (4.955 m^3s^{-1}) is used to drive the

---

* Graduate Research Assistant and AIAA Student Member.

† Associate Professor of Mechanical Engineering, 1700 West Third Avenue, and AIAA Associate Fellow.

flow. A 20-inch by 20-inch honeycomb section, 0.5-inch thick, is used to reduce the turbulence from the blower. From there the flow is contracted over the course of 4 feet in streamwise length, from 20 inches square at the blower to 12 inches square at the test section. The top of the test section is hinged for access to the model, and a set of access ports are available to run lines for wiring and pressure. Due to past tests done using this wind tunnel, the model to be tested (in this case, a flat plate) is placed horizontally across the width of the tunnel, with the DBD actuator sitting on top of it. The actuator design is discussed in greater depth in the next section. The flow exits the wind tunnel after passing through a diffuser identical to the contraction, placed in reverse. Figure 1 shows the CPDL Wind Tunnel and the test section setup.

Fig. 1: CPDL experimental facility wind tunnel (left) and the setup of the test section (right).

The base geometry tested was a flat plate constructed out of a 0.5-inch thick piece of smooth polycarbonate. The span of the plate was 6 inches, and the streamwise length was 1 foot. It featured a leading edge beveled at 30^{o} from the vertical and had a single-pair DBD actuator attached 50 mm from the leading edge. Static pressure taps in the top of the flat plate fed into lines of pressure tubing, which then ran into the DSA unit. Table 1 below shows the tap location with respect to the trailing edge of the DBD actuator. The locations for these taps was based on work originally performed by Volino and Hultgren [7] and later by Hultgren and Ashpis [8], converted to metric units with the fractional millimeters ignored.

Table 1: Pressure tap locations on the flat plate, measured from the trailing edge of the actuator.

Tap Number	1	2	3	4
X-location from actuator (mm)	58	69	81	95
Tap Number	5	6	7	8
X-location from actuator (mm)	105	119	131	144

Pressure measurements were made using a Scanivalve DSA 1732 Intelligent Pressure Sensor and were communicated to a data acquisition computer via an Ethernet crossover cable. The DSA has sixteen pressure leads, though only as many as nine were used at any one time.

The measurements for the C_p curves were made separately from the measurements for the velocity profiles. A pitot-static probe was used to capture these initial velocity profiles, as well as the free-stream static pressure used in calculating C_p. The pitot tube was affixed to the outside roof of the test section by means of a clamp holding a fin (to which the pitot assembly was attached) to a runner on the top of the test section. The runner was placed alongside a slot so that the pitot assembly could be traversed streamwise down the length of any given model, and both the fin and the runner were marked with 1-mm spaced hashes to provide a basis for accuracy and precision.

The humidity tests were run using regular tap water, delivered by a Brookstone ultrasonic humidifier. The output vent of the humidifier was directed into the rear of the fan, alongside the electric motor to prevent water from being sucked into the motor's cooling ports (and possibly shorting it out).

2.2 Actuator

The plasma actuator was placed 50 mm from the leading edge of the flat plate. It consists of a dielectric layer (Kapton film layers 2.5 mils thick) sandwiched between two thin copper electrodes arranged asymmetrically. This asymmetric arrangement of the electrodes is based on findings by Enloe et. al. [9]. Figure 2 below shows a cross-sectional view of our DBD single-pair device. Figure 3 beneath it shows a planform photograph of the device as attached to the flat plate and wired for operation.

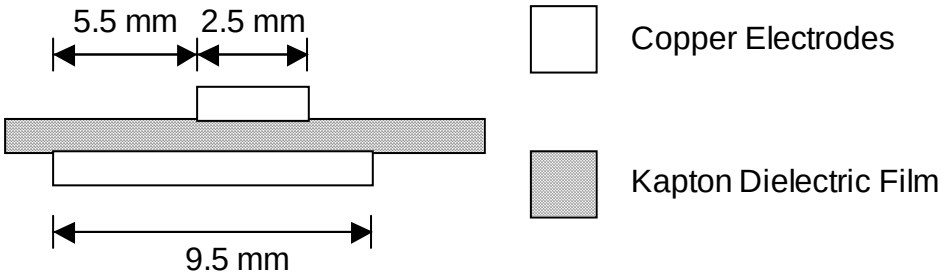

Fig. 2: Cross section view of the DBD actuator used in humidity experiments (not to scale).

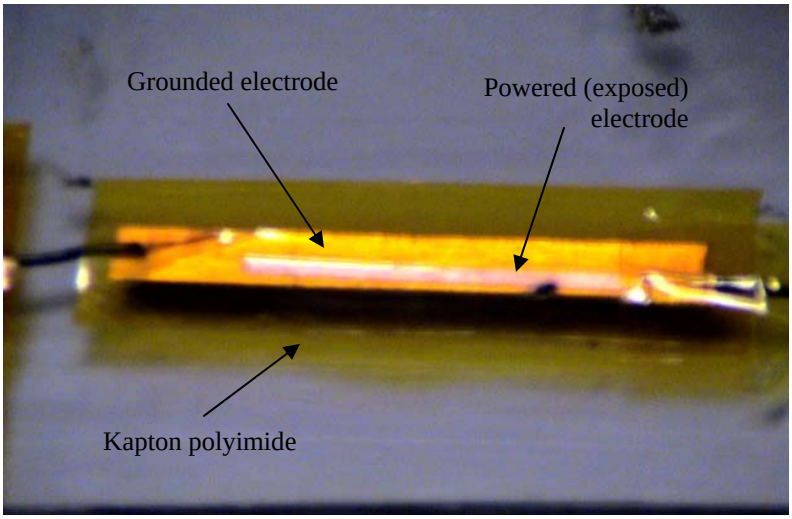

Fig. 3: Planform photograph of the DBD actuator in operational setting.

The length of the lower electrode was 9.5 mm; the upper electrode measured 2.5 mm long. The useful span of the actuator was 35 mm, despite the fact that each electrode had a 60 mm span. The leads of the wires used to power the circuit took up the remaining 25 mm. The device was powered from wall current at 120Vrms and 60 Hz, which was then fed to a Franceformer 12030 H transformer. This transformer was originally intended for use ionizing neon sign gasses, and required only slight modifications on the output terminals to make suitable for DBD use. The secondary of the transformer delivered 30 mA at 12 kV and 60 Hz to the upper electrode of the actuator on the top surface of the flat plate, for a total power draw of 360 Watts. The lower electrode was connected to an earth-ground. It should be pointed out that this is a crude design for a DBD device, and that improved results may obtain from using a more efficient actuator design. Figure 4 below shows the DBD actuator in use, with bluish glow around the exposed electrode indicating the span of the discharge. The original glow picture taken with a regular video camera was dim. The zoomed in picture shown below was enhanced using adaptive lighting and hue enrichment. The blackened gap located towards the right (separating glow) indicates a region where a Kapton patch is used to help position the wiring.

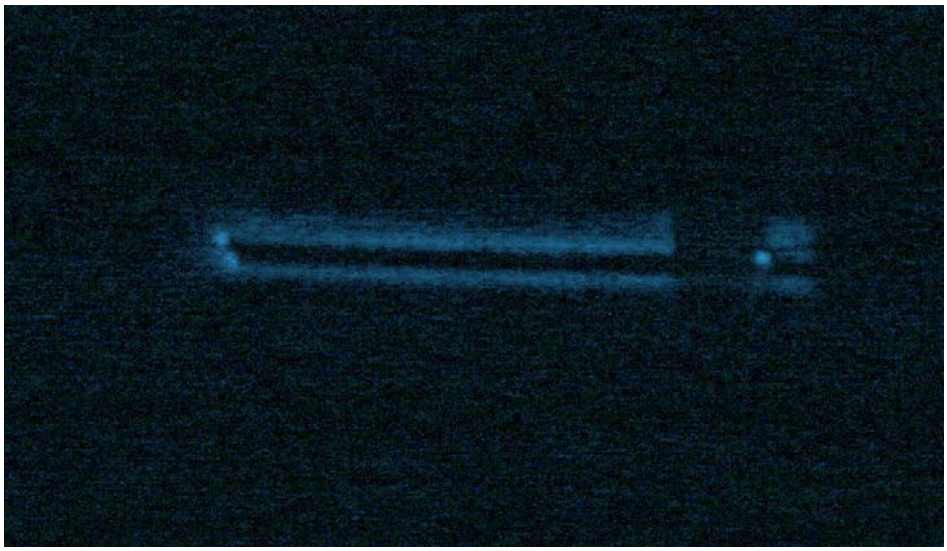

Fig. 4: Operational photograph of the DBD actuator.

3. Results

3.1 Pressure Coefficients

The tests conducted represent a wide initial variety of free-stream velocities and relative humidities. Based on past calibrations, the fan was run at speeds of 900, 1700, and 2400 rpm. These fan speeds correspond roughly to 5, 10, and 15 ms^{-1}. All humidity tests were performed using the "high" volume setting, and a dial regulated the humidity as appropriate for each test. The RH was varied from approximately 43% with the humidifier off to 53% with the highest humidity setting. An intermediate setting on the humidifier also delivered a 48% RH for the midlevel humidity tests. Change in actuator effectiveness is taken to be the change in absolute pressure coefficient at any given humidity level.

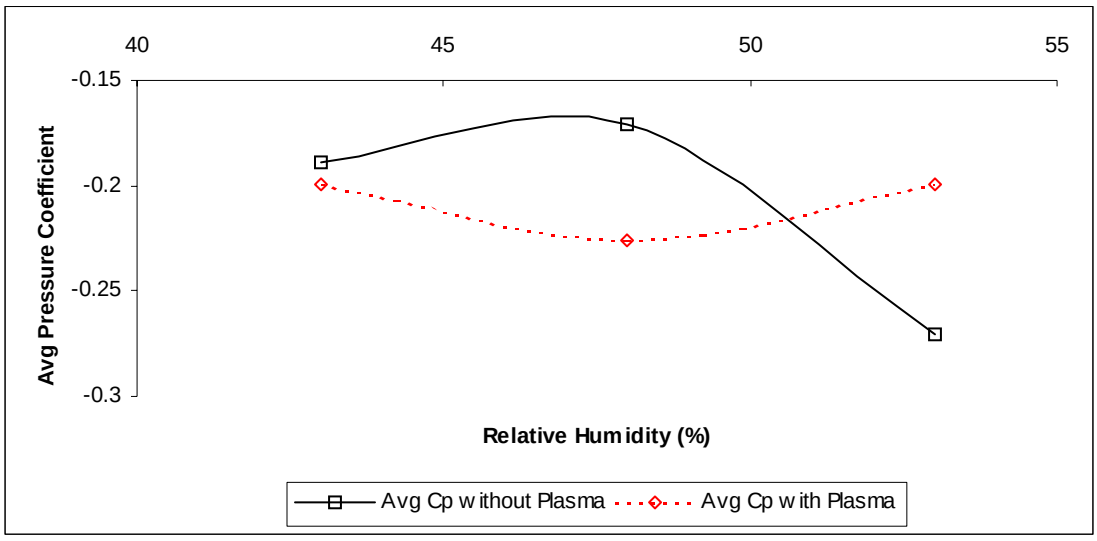

Fig. 5: Average pressure coefficient plotted as a function of relative humidity, with fan at 900 rpm.

Figure 5 above shows the average value of the C_p compared with the RH for each test. The average was calculated from 40 C_p measurements at each operational condition (actuator operation and RH level) with a constant setting of 900 rpm on the fan, which corresponds to a flow speed of approximately 5 ms^{-1}. It should be pointed out that the anticipated falloff in performance of a DBD in a higher-humidity environment is present, but small. More importantly, this chart presents the greatest outlier in the data. After an initial gain in actuator effectiveness (as seen by the increase in absolute value of the pressure

coefficient) at the 48% RH level, the actuator effectiveness decreases to a level only slightly greater than the lowest humidity setting. However, unlike any other run in this sequence of experiments, at 5 ms^{-1} the actuator-off test has the greater absolute Cp than the actuator-on case at the highest humidity.

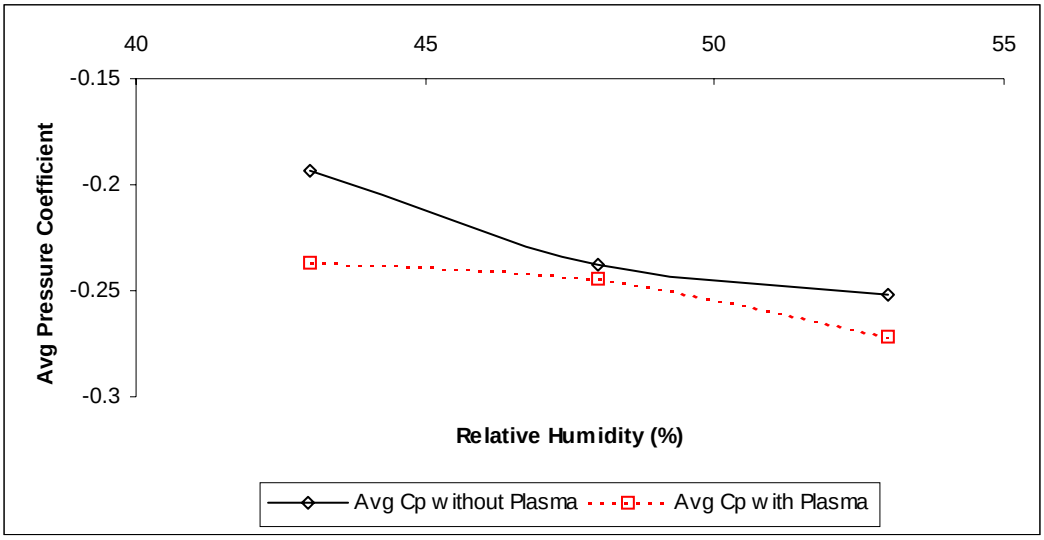

Fig. 6: Average pressure coefficient plotted as a function of relative humidity, with fan at 1700 rpm.

As seen in Figure 6 above, the tests performed with a free-stream velocity of roughly 10 ms^{-1} are much better at providing an example of the trend of the correlation between humidity and C_p induced by a DBD actuator. From 43 to 48% RH, the active-actuator case remains nearly constant, as compared with the greater increase in absolute Cp shown by the actuator-off case. As the RH level is increased a further 5%, this relationship is reversed, with the greater impact showing in the active DBD tests. Interestingly, this plot shows an increase in actuator effectiveness (as measured by absolute C_p) as the RH increases. As seen for the highest fan setting, this increase is the general trend.

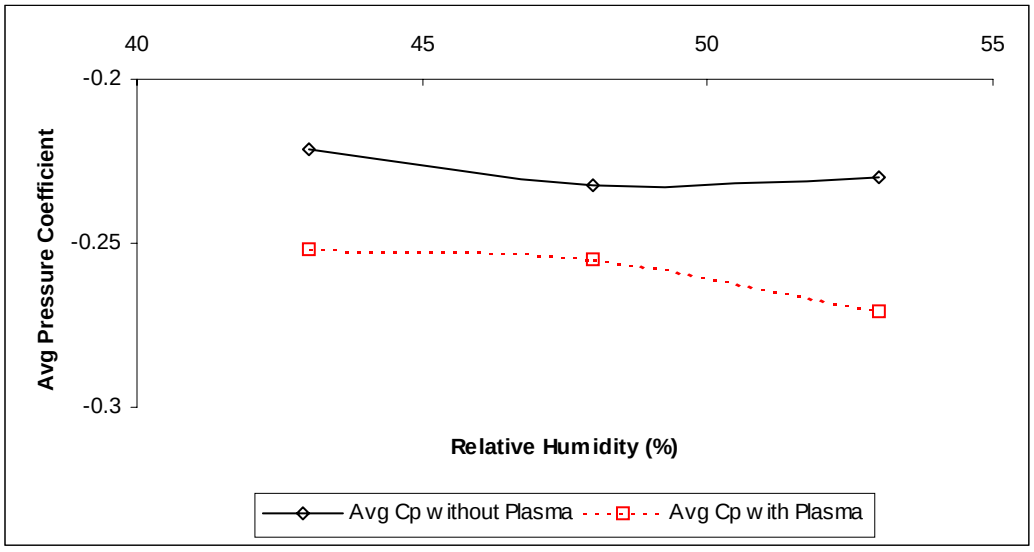

Fig. 7: Average pressure coefficient plotted as a function of relative humidity, with fan at 2400 rpm.

The first thing that should be noticed from Figure 7 above is that the trend shown at the 10 ms^{-1} flow speed appears to continue at the new fan setting, corresponding to approximately 15 ms^{-1}. Not only does the actuator effectiveness increase as the humidity increases, it also increases at a greater rate between 48% and 53% RH than between 43% and 48%. Furthermore, the actuator effectiveness, as indicated by the

average value of the absolute C_p, is greater across the board at the higher flow speed. This suggests that the increase may have a component from the free-stream velocity as well as one from the RH.

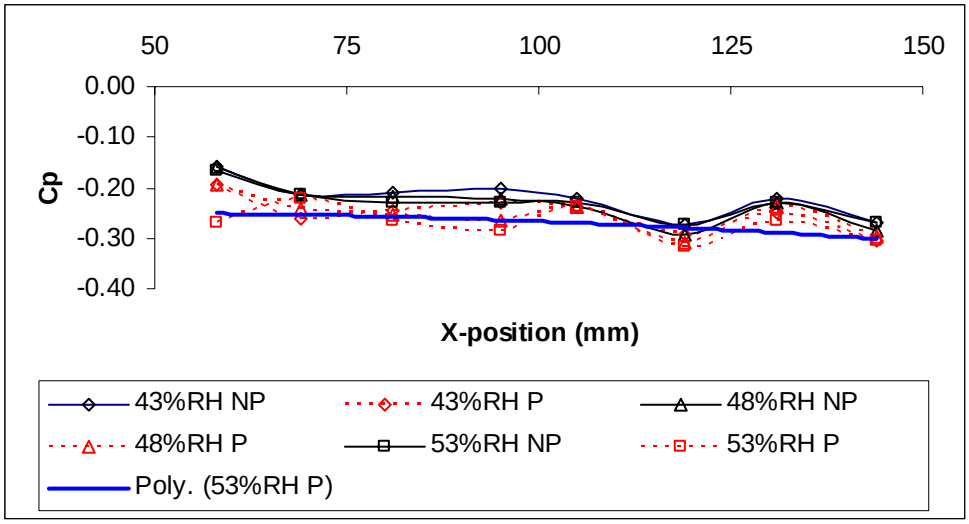

Fig. 8: Pressure coefficient plotted as a function of downstream position from the actuator trailing edge, with fan at 2400 rpm.

Above is Figure 8, the final plot of the pressure coefficient series of experiments. Again it shows the fan setting of 2400 rpm, corresponding to a flow speed of approximately 15 ms^{-1}. In this case, however, it shows the positional C_p value (as opposed to the average of these values, shown in Figs. 5–7). The trendline (the thick solid line) corresponds to the 53% RH tests run with the actuator on. Of the eight positions, the 53% RH active-actuator test has three points with a greater absolute C_p than the other active-actuator tests, one with a reduced absolute C_p value, and four that are roughly common to all three active-actuator series. The farthest departure for the 53% RH active actuator test from any equivalently-positioned active actuator test is approximately 27%. Furthermore, the variance reduces as the distance from the actuator increases, which is a well-expected result suggesting that actuator effectiveness is reduced as the downstream distance from the actuator increases. The variance in absolute C_p is such that further tests are needed to solidify our results, but due to the low base values for the plate C_p, we can safely state that the operation of the DBD actuator should not be greatly inhibited by relative humidities extending into the lower 50^{th} percentile.

3.2 Friction Coefficient

Using the Reynolds number of the flow, and the Blasius approximation for the friction coefficient as found in reference [10], we attempt to calculate the theoretical value for C_f, the friction coefficient using the equation $C_f = 0.664/\mathrm{Re}^{0.5}$.

Velocity tests were made with a pitot-static probe at positions 3 and 4 on the flat plate. Due to the physical size of the pitot probe, measurements were made only as close as 4 mm from the wall. Three measurements of velocity were made for each of the six major conditions (two states of the DBD actuator at each of the three RH levels). Due to past studies in the literature [1, 8], it was initially assumed that the DBD actuator causes a turbulent boundary layer downstream. This supposition is disproved in our tests by calculations of the Reynolds number based on the average velocity at the x-positions we have investigated for this particular section. The calculated Reynolds numbers are consistently lower than $2x10^5$, below the Reynolds value generally thought of as indicative of turbulent flow. While this value could be in the transitional regime, inducing unsteady waves, for simplicity in the preliminary calculation the laminar version of the friction coefficient equation is used [10].

Above is Figure 9, which shows the calculated values for the friction coefficient for both the active and inactive actuator cases at all three fan settings. This plot suggests that the friction coefficient is reduced by distance from the actuator more than humidity, but that humidity does play a role in reducing the friction coefficient (and thus the overall drag on the body), at flow speeds greater than 10 ms^{-1}.

Interestingly, these results are not obtained for the 900-rpm fan setting (roughly equivalent to 5 ms^{-1}), as shown in Fig. 9-a. Even more interesting is the fact that the medium RH setting (48%) had a generally higher C_f value than either extreme. This suggests that there might be an optimal operating point for the humidity with respect to increased drag—a point that operators would usually prefer to avoid. Furthermore, at only one operating point is the C_f value for 53% RH higher than for 43% (Fig. 9-a, tap 3). This suggests that humidity has an effect on the operation of the DBD actuator with respect to any theoretical drag reduction.

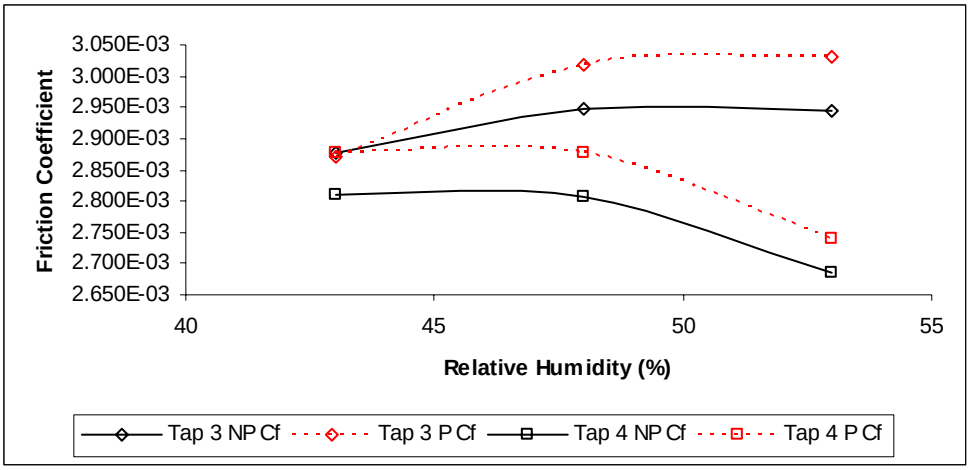

(a)

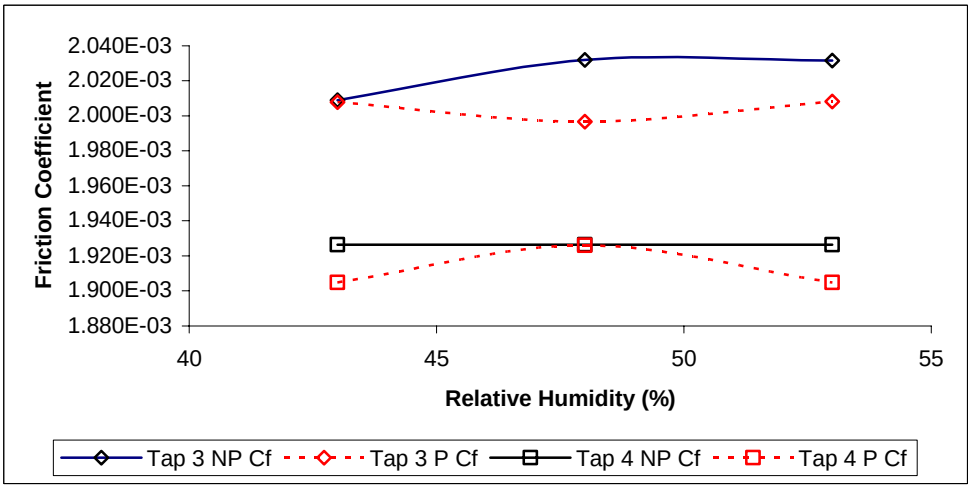

(b)

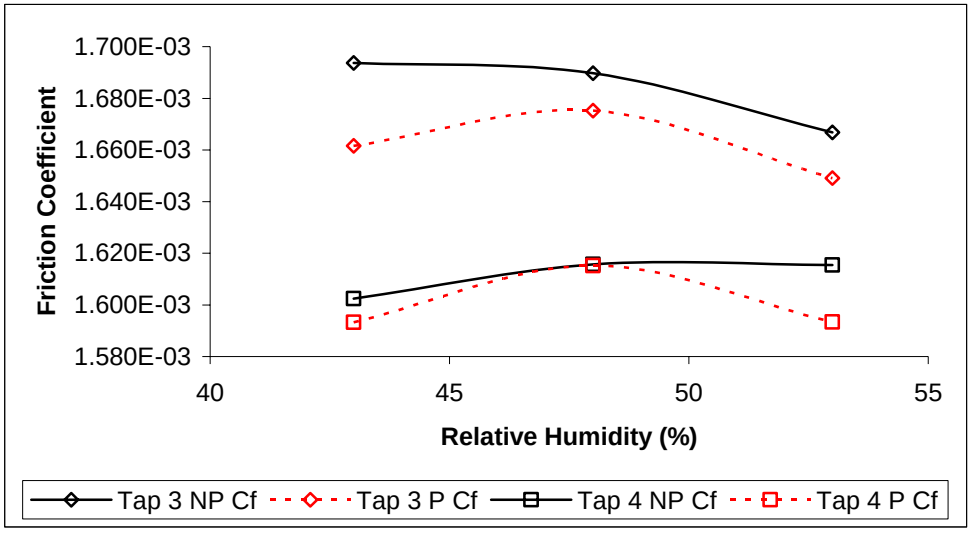

(c)

Fig. 9: Plot of friction coefficient for active and inactive DBD actuator against RH level at x-positions 3 and 4 at fan settings of (a) 900 rpm, (b) 1700 rpm, and (c) 2400 rpm.

4. Summary

Initial results are shown for testing DBD flow control actuators across four flow speeds (including one for the quiescent flow). Evidence is cited suggesting that the operation of the DBD actuator for purposes of flow control is possible at RH levels extending as high as 53%. Additional data suggests that the effectiveness of the actuator is increased as RH increases, and that this increase may be enhanced in the region nearest the actuator. Further investigation is needed to validate these results. Particular attention for any future studies would include reducing the oscillation of positional C_p values shown in this Fig. 8 of this study (a result of flow unsteadiness or the onset of transition to turbulence), as well as determining the critical levels of humidity, if any, for possible shutdown of plasma generation and its impact on flow control.

The friction coefficient, a component of drag, is calculated for the flat plate at two positions downstream of the DBD actuator. While a greater reduction in Cf may be attributed to position than humidity, in only one of six tests is C_f increased with increasing RH. In half of the tests, Cf is reduced with increased humidity, and in the remaining two the value of C_f returns to the same value as at the initial RH level. In all cases except one, increased C_f (and thus drag) was experienced at the intermediate RH level as compared with the extreme values. This should be kept in mind for future operations of the DBD actuator.

Future experiments in this direction should be performed using hot-wire or hot-film anemometers to eliminate the wall proximity limitations of the pitot-static probe used here. Additionally, more data points are needed to corroborate or refute these preliminary results, with particular emphasis on a greater range of RH values. Lastly, improved DBD device geometries should also be tested with respect to their operability in humid atmospheres.

Acknowledgements

The authors would like to acknowledge the following for their contributions to this project: Dr. K. Joel Berry for his consistent support throughout the development of the CPDL Test Facility; Prof. B. Lemke and Dr. R. Chandaran for their discussions regarding instrumentation; Dr. H. Hiziroglu for his discussions regarding safety, operation, and construction of high-voltage circuits; Dr. K.P. Singh and Mr. H. Kumar for their assistance in the operation of the CPDL Test Facility; Dr. R. Rivir and Dr. D. Gaitonde, for discussions regarding plasma actuators in general, and specifically on physical and numerical experiments with them respectively. The first author would also like to thank the Air Force Research Laboratory for the VAAC Summer Graduate Student fellowship during 2005.

References

[1] Corke, T., C. He, and M. Patel. 2004. "Plasma Flaps and Slats: An Application of Weakly-Ionized Plasma Actuators." *AIAA Paper 2004-2127*.

[2] Roth J. *"Method and Apparatus for Covering Bodies with A Uniform Glow discharge Plasma and Applications Thereof."* U. S. Patent # 5,669,583, Issued Sept 23, 1997.

[3] Jacob, J., K. Ramakumar, R. Anthony, and R. Rivir. 2005. "Control of Laminar and Turbulent Shear Flows Using Plasma Actuators" TSFP4-225, Fourth International Symposium on Turbulence and Shear Flow Phenomena, Williamsburg, Virginia, June 27-29, 2005.

[4] Roth J.R. 2003. "Aerodynamic Flow Acceleration using Paraelectric and Peristaltic Electrohydrodynamic (EHD) Effects of a One Atmosphere Uniform Glow Discharge Plasma." *Physics of Plasmas*, Volume 10, No. 5.

[5] Borghi, C., M. Carraro, and A. Christofoline. 2005. "Plasma Characterization of a One Atmosphere Uniform Barrier Discharge." *AIAA Paper 2005-1179*.

[6] Mehta, R. and P. Bradshaw. 1979. "Design rules for small low speed wind tunnels." *Royal Aero. J.* Volume 83, Page 443.

[7] Volino, R. and L. Hultgren. 2001. "Measurements in Separated and Transitional Boundary Layers Under Low-Pressure Turbine Airfoil Conditions." *J. Turbomachinery* Volume 123, Pages189-197.

[8] Hultgren, L. and D. Ashpis. 2003. "Demonstration of Separation Delay with Glow-Discharge Plasma Actuators." *AIAA Paper 2003-1025*.

[9] Enloe, C., T. McLaughlin, R. VanDyken, K. Kachner, E. Jumper, T. Corke, M. Post, and O. Haddad. 2004. "Mechanisms and Responses of a Single Dielectric Barrier Plasma Actuator: Geometric Effects." *AIAA Journal* Volume 42, Pages 595-604.

[10] Cengel, Y. and J. Cimbala. 2006. *Fluid Mechanics: Fundamentals and Applications*. McGraw-Hill, New York.